Small-core chalcogenide microstructured fibers for the infrared

Frédéric Désévédavy,[1,5] Gilles Renversez,[2,*] Laurent Brilland,[3] Patrick Houizot,[1] Johann Troles,[1] Quentin Coulombier,[1] Frédéric Smektala,[4] Nicholas Traynor,[3] and Jean-Luc Adam[1]

[1]Laboratoire Verres et Céramiques, UMR CNRS 6226, Université de Rennes 1, Rennes, France

[2]Institut Fresnel, UMR CNRS 6133, Université d'Aix-Marseille, Marseille, France

[3]PERFOS (plateforme d'Etudes et de Recherche sur les Fibres Optiques Spéciales), 11 rue Louis de Broglie 22300 Lannion, France

[4]Institut Carnot de Bourgogne, ICB UMR CNRS 5209, Université de Bourgogne, Dijon, France

[5]frederic.desevedavy@univ-rennes1.fr

*Corresponding author: gilles.renversez@fresnel.fr

Received 1 August 2008; revised 7 October 2008; accepted 13 October 2008; posted 13 October 2008 (Doc. ID 99575); published 4 November 2008

We report several small-core chalcogenide microstructured fibers fabricated by the "Stack & Draw" technique from $Ge_{15}Sb_{20}S_{65}$ glass with regular profiles. Mode field diameters and losses have been measured at 1.55 μm. For one of the presented fibers, the pitch is 2.5 μm, three times smaller than that already obtained in our previous work, and the corresponding mode field diameter is now as small as 3.5 μm. This fiber, obtained using a two step "Stack & Draw" technique, is single-mode at 1.55 μm from a practical point of view. We also report the first measurement of the attenuation between 1 and 3.5 μm of a chalcogenide microstructured fiber. Experimental data concerning fiber attenuation and mode field diameter are compared with calculations. Finally, the origin of fiber attenuation and the nonlinearity of the fibers are discussed.

OCIS codes: 160.2750, 060.2310, 060.2270, 060.2280.

1. Introduction

To extend the wavelength range available for light guiding in microstructured fibers (MFs) toward the midinfrared is a challenging task, which would allow the extension of techniques successfully used between 0.5 and 1.7 μm to longer wavelengths [1,2]. At least two bands are of particular interest, from 3–5 μm and from 8–12 μm due to low atmospheric absorption, for applications such as light-imaging detection and ranging (LIDAR), or hyperspectral imaging. Other applications, such as supercontinuum generation [3,4] or sensors [5,6], may also be envisaged. To reach such goals, chalcogenide glasses are doubtlessly good candidates due to their low bulk material losses in the midinfrared spectral region and to their high nonlinear coefficient [7,8]. Only a few chalcogenide microstructured fibers have already been reported in the literature because fiber fabrication has proved to be an extremely difficult technical task. The first report concerned an irregular structure obtained by extrusion and made of only one ring of holes [9] and where no optical characterization was given. More recently, we have shown by using the chalcogenide glass 2S2G ($Sb_{10}S_{65}Ge_{20}Ga_5$) that the "Stack & Draw" procedure is a useful tool to build complex and regular MFs made of several rings of holes [10]. In this previous study, no attenuation measurement could be realized due to the strong

0003-6935/08/326014-08$15.00/0

losses of the fibers, and the smallest pitch obtained was 7.7 μm. Furthermore, only a multimode MF was obtained. In the work presented here, we describe the fabrication, characterization, and modeling of MFs made of chalcogenide glasses from the system Sb-S-Ge (2SG). This glass was chosen to allow a reduction in the overall losses of the fabricated MFs. The glass losses are given from 1.5 up to 7.5 μm with a minimum of 0.05 dB/m at 2.3 μm and with a value of 0.39 dB/m at 1.55 μm. To the best of our knowledge, no such results have already been published for this glass. The overall MF losses are measured at 1.55 μm for all three fabricated MFs, and a full attenuation curve is given from 1 to 3.5 μm for one of the fibers. We also describe the first chalcogenide small solid core MF (mode field diameter less than 4 μm) that exhibits single-mode behavior at 1.55 μm. This MF was obtained using a two step drawing technique and its pitch is 2.5 μm, which is more than three times smaller than that previously obtained. Its effective area is measured at 10 μm^2, which is seven times smaller than the one previously reported [10]. The main application of such a MF would be nonlinear based devices such as a supercontinuum sources in the midinfrared [11,12]. In the present study, we also give numerical results concerning mode field diameters and attenuation computed with or without material losses. Good agreement between calculations and experimental data is obtained for the three considered MFs, allowing us to define some practical rules to improve future fabrication. To the best of our knowledge, no such comparisons have already been published previously for chalcogenide MFs. It is worth mentioning that the first two fibers we present are necessary for the present study notably because they enable a better understanding of the origins of the overall losses in chalcogenide MF obtained with the "Stack & Draw" procedure. Loss issues are much more crucial in chalcogenide MF than in silica ones in which the losses are already at the dB/km level [13–15].

The article is organized as follows: in Section 2 glass synthesis is described. The fabrication and characterization of a 2SG monoindex rod are described in Section 3. The description of fiber fabrication and their geometrical characterization is given in Section 4. Section 5 deals with optical characterization of the three MFs with optical losses and mode field diameters compared to numerical simulation results. Finally, the origins of the overall losses are discussed in Section 6, first using numerical simulations and second considering fabrication issues. The single mode behavior of the MF with the smallest core at 1.55 μm is demonstrated using numerical simulations. In Section 6 we also evaluate the effective nonlinearity in this small-core chalcogenide MF.

2. Glass Synthesis

Among the wide variety of chalcogenide glasses, we have selected the 2SG ($Sb_{20}S_{65}Ge_{15}$) glass because it presents a good compromise between its linear and nonlinear properties. The index of refraction is 2.37 at 1.55 μm, and the n_2 is very similar to that of the 2S2G glass (3.2 10–18 m^2/W at 1064 nm, 120 times higher than that of silica glass) [10]. The glass is transparent for bulk samples between 600 nm and 11 μm, giving the glass a red color. The phonon energy of this chalcogenide glass is around 350 cm^{-1} [16]. The partial transparency of this material in the visible is a useful aid for the glass and fiber fabrication process, as eventual defects such as bubbles, crystals, and refractive index variations can be easily visualized. This is not the case when working with selenide or telluride based glasses, which are opaque in the visible wavelength region. In our previous work [10], we have used another sulfide glass from the Sb-S-Ge-Ga system. The current compositional change is mainly due to the purification process for this glass, which enables a decrease of the global fiber loss (see Section 3). The previous glass suffered from the inclusion of gallium, which has a low vapor pressure, meaning that complete distillation of 2S2G glass is not possible. The absence of gallium from the current glass removes this problem. The degree of purity of the final material is determined by the content of impurities in the constituent elements, by introduction of impurities from the apparatus walls and by contamination of the batch components during their loading into the silica tube where the glass is synthesized. The glass is prepared from high purity raw materials (5N: 99.999%): antimony, germanium, and sulfur are supplied by Alfa Aesar, Umicore, and Strem, respectively. However the sulfur used still has high levels of OH, water, and carbon. The required amounts of the different elements are placed in a silica ampoule under vacuum (10^{-5} mbar). Then the sulfur is purified using dehydration and distillation procedures. After sealing, the ampoule is introduced in a rocking furnace and progressively heated up to 800 °C. The ampoule is maintained at this temperature for 12 h, before being quenched in water to allow glass formation and avoid any crystallization process. The vitreous sample is then annealed for several hours at the glass temperature (Tg = 250 °C) to relax the internal mechanical stress induced by quenching, and it is slowly cooled to room temperature. A glass rod is subsequently obtained.

3. Shaping of the Glass and Monoindex Optical Fiber Fabrication

The realization of microstructured optical fibers requires the preparation of glass tubes. One glass tube is used for the fiber jacket and another is used to draw the capillaries that will form the holes of the fiber. Tubes are fabricated by centrifugation of a 700 °C glass melt spinning at 3000 rpm at ambient temperature during several minutes (see Fig. 1). During the rotation cooling occurs, the viscosity increases, and the formation of a vitreous tube is obtained after a few minutes. The glass rod is obtained as described in the Section 2.

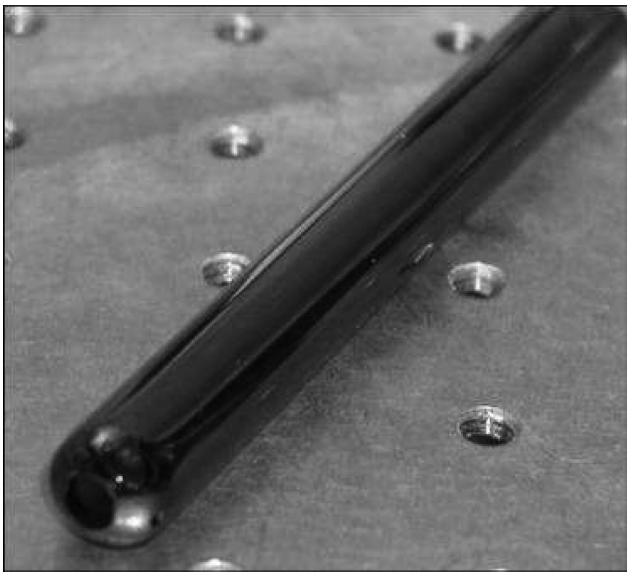

Fig. 1. Chalcogenide glass tube.

Before the fabrication of the MF, we have drawn a single index fiber from the previous glass rod to control its quality by measuring the optical losses. The material losses of the monoindex fiber have been measured using the cutback technique with a Fourier transform infrared spectrometer (Bruker) from 1.5 to 8 μm. Figure 2 shows the typical attenuation curve of 2SG glass single index fiber after purification, obtained via cutback on 20 m of fiber. Several extrinsic absorption bands are present, especially those associated with the S–H vibration at 4 and 3.1 μm, which are due to a reaction between the glass and the remaining water in the batch. The carbon particles and water that are present in the initial sulfur are not completely removed during the purification process. The extinction coefficient of the S–H band is equal to 2.5 dB/m/ppm [17], which means that the quantity of S–H in our glass is below 5 ppm. The presence of remaining carbon particles that induce strong scattering behavior [18] explains the increasing loss observed below 2 μm. The losses above 6 μm are induced by oxides and multiphonon absorptions. The losses at 1.55 μm are equal to 0.39 dB/m. The minimum attenuation is 0.05 dB/m around 2.30 μm. The reduction of the S–H absorption band to a reasonable level opens up significant transmission windows in the 3–5 μm region of interest, notably between 4.5 and 5 μm, as well as between 3 and 3.8 μm, with attenuation below 0.5 dB/m. The low loss level reached for the measured attenuation spectrum justifies the choice of the 2SG glass.

To ensure the refractive index homogeneity of the microstructured area, it is necessary that this zone is made with identical glass. We therefore draw the core rod for the MF from the same 2SG tube used for capillaries, collapsed by drawing in a negative pressure regime. As a consequence, the material losses of a monoindex fiber made from this rod are increased from the intrinsic losses, and are measured to be 4.26 dB/m at 1.55 μm, 2.4 dB/m at 2.5 μm, and 2 dB/m at 5 μm. The origin of this loss increase is the same as the origin of the increased loss observed for the fabricated fibers, as described in Section 6. Each MF presented here is made of capillaries and core rods originating from the same glass batch.

4. Microstructured Fiber Fabrication

The fabrication of the MF is realized through the "Stack & Draw" technique which consists of the fabrication of a preform presenting the required geometrical arrangement of air holes around a solid glass core [10,19,20]. Capillaries are stacked in a triangular lattice around the solid core rod of identical diameter, and placed in a larger jacket tube to create the preform. To exacerbate nonlinear effects a small-core diameter is needed [21,22]. To decrease the core size, a microstructured cane with a diameter of 3 mm is drawn from the previous preform and is then inserted into a second jacket tube of 4 mm inner diameter (see Fig. 3). The jacket tube is collapsed onto the microstructured rod and this preform is drawn again, down to the final optical fiber. In this way the core/clad diameter ratio is reduced without reducing the overall fiber diameter. We call this process the two step "Stack & Draw" technique as opposed to direct fiber draw from the initial preform (one step "Stack & Draw" technique).

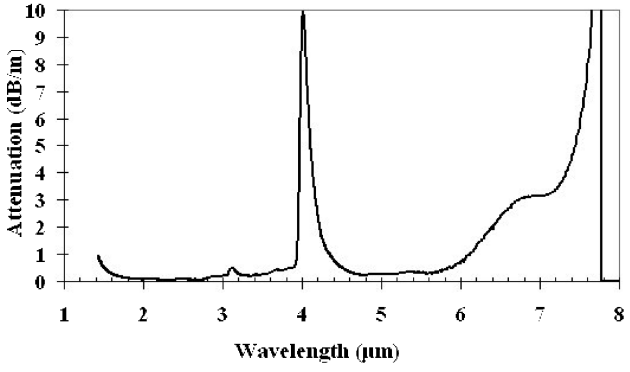

Fig. 2. Typical attenuation curve of 2SG glass monoindex fiber, $\Phi_{ext} = 400\,\mu$m.

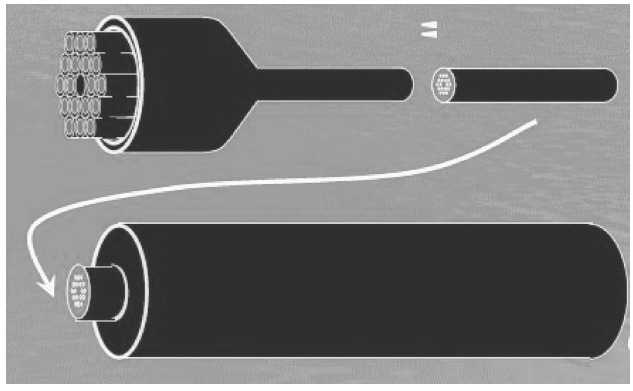

Fig. 3. Jacketing of the stack, drawing and jacketing of the microstructured stick to get small-core MF.

Table 1. Summary of the Different Drawings

Fiber	Process	Φ_{fiber} (μm)[a]	d (μm)	Λ (μm)	Deduced d/Λ ratio	Losses (dB/m) at 1.55 μm
MF1	One step stack and draw technique	150	4.7	11.1	0.423	13
MF2a	One step stack and draw technique	275	6.0	14.0	0.429	15
MF2b [b]	Two step stack and draw technique	150	1.07	2.5	0.429	34

[a] Φ_{fiber} is the fiber outer diameter. The losses are measured with monochromatic light at 1.55 μm.
[b] For fiber MF2b, the value of the hole diameter d has been estimated from the measured pitch and the measured d/Λ ratio of the MF2a, the measured value of the diameter being 1.1 μm (see the text for the details).

It is well known that the high index of refraction of chalcogenide glass enables a better confinement of light in conventional solid core MFs compared to silica. While the number of rings can be reduced for an equivalent core size, several rings are nevertheless necessary to reduce the confinement losses to below the intrinsic glass loss [10,23]. Our previous work [10] shows that, in many cases, three rings of holes are sufficient to ensure guiding losses below material losses of around 1 dB/m. In the present paper we report the fabrication of small-core MFs from 2SG glass with structures based on three rings of holes. Table 1 summarizes the fabrication process and the geometrical specifications of each fiber. Three different fibers have been studied, MF1, MF2a, and MF2b.

Figure 4 shows the cross section of fiber MF1, with three rings of holes (Nr = 3). The outer diameter (Φ_{ext}) is 150 μm, the distance between hole centers (pitch) is $\Lambda = 11.1\,\mu$m, the average hole diameter is 4.7 μm, and the deduced ratio d/Λ is 0.423. The average size of the triangular interstitial holes is 1.2 μm.

One can observe from Fig. 4 that interstitial holes are present across the fiber cross section. These extra holes come from the spaces which exist between the capillaries when they are stacked. The collapse of the external tube was not sufficient in this case to close these holes during the jacketing step of the fabrication of the preform. A second three hole ring MF was realized (MF2a) with an outer diameter Φ_{ext} of 275 μm, a pitch Λ of 14 μm, an average hole diameter of 6 μm, and an estimated ratio of d/Λ at 0.429. The preform used for fiber MF2a was subsequently drawn down to form a cane and jacketed with a second 2SG tube to decrease the core/cladding diameter ratio (Fig. 3). The obtained preform was drawn under the same atmosphere and temperature conditions as MF2a. This fiber (fiber MF2b) is represented in Fig. 5, together with a zoom of the microstructured region. The characteristics are $\Phi_{\text{ext}} = 150$, $\Lambda = 2.5\,\mu$m. This pitch is three times smaller than that of fibers obtained in our previous work [10]. The measured hole diameter d is 1.1 μm with a relatively high uncertainty. Other fiber draws with similar structures and using the same draw conditions have shown that the d/Λ ratio is conserved in the process used to draw MF2b from MF2a. Using the d/Λ ration of M2a (0.429), we estimate a d value of 1.07 μm using the measured pitch of 2.5 μm, in agreement with the above value. The measured core size is 4 μm.

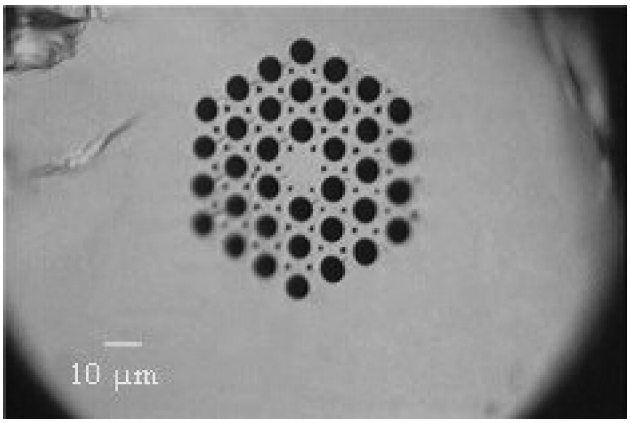

Fig. 4. Picture of the cross section of 2SG fiber MF1.

The two vertical lines at the bottom of Fig. 5 (left) are due to the transversal breaking of the fiber when it was cleaved before analysis. The large hole visible in the lower part of the holey cladding is explained by the presence of an interstitial hole between the stack and the external tube before the jacketing step. The collapse of the external tube was not sufficient in this case to close this hole. Moreover these holes at the edge of the holey region, are the largest of the preform in this kind of stack, and the gas pressure used during the drawing of the fiber leads to their growth. One can note that the third ring is not complete.

5. Optical Characterization and Modeling Results

Optical measurements were made on the fibers using near-field microscopy. An indium metal coating was applied to inhibit cladding mode guidance. Monochromatic light ($\lambda = 1.55\,\mu$m) guided in a single-mode silica optical fiber is butt-coupled to the 2SG MF. The typical fiber length used for the measurements was 50 cm. The image of the fiber output was visualized on an IR camera (Electrophysics) as shown in Figs. 6, 7(a), and 7(b). The output profiles can be accurately fitted with Gaussian functions.

The mode field diameter (MFD) of MF1 at $1/e^2$ of maximum intensity of the fundamental mode is measured using a Gaussian curve fitted to the mode profile [see Fig. 8(a)]. Along the x axis, the measured value is 11.0 μm, while the expected value calculated based on the fiber geometry is 10.7 μm, representing a relative error of 3%. Along the y axis, the measured value is 12.2 μm, versus a calculated value of 11.3 μm, representing a relative error of 8%. We believe that the source of these discrepancies can be at least partially explained by uncertainty in the measured size of the triangular interstitial holes. Attenuation

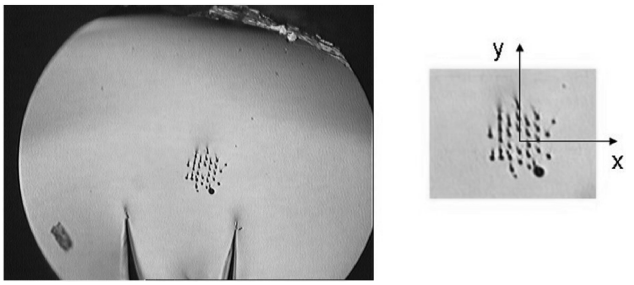

Fig. 5. Picture of the cross section of 2SG fiber MF2b, $\Phi_{core} = 4\,\mu m$.

for this fiber was measured to be 13 dB/m at 1.55 μm using the cutback method on a 50 cm fiber length. For the numerical simulations, it is possible to compute the overall losses with and without taking into account the material losses. For the fundamental mode at 1.55 μm, the computed losses are around 10^{-2} dB/m without material loss and 4.35 dB/m with material loss. The measured loss is 8.5 dB/m above this minimal threshold. We discuss in Section 6 the reasons for this difference.

For the second mode at the same wavelength, the computed losses are approximately equal to 0.14 dB/m (without material losses) whereas they are around 4.57 dB/m with them. The similar level of computed losses of the fundamental mode and of the second mode explains why this higher order mode was easily observed [see Fig. 8(b)]. To the best of our knowledge, this figure represents the first second mode profile observed in a chalcogenide MF.

The measurement of optical attenuation for MF2a at 1.55 μm was made using the same technique as for MF1. The attenuation value at 1.55 μm has been found to be 15 dB/m measured by the cutback method on 50 cm of fiber. The losses have also been recorded between 1 to 3.5 μm using a sensitive FTIR spectrometer (Thermo Electron 5700) adapted to small-core fiber (see Fig. 9). The image of the fiber output is visualized on a thermal camera (FLIR) working from 3 to 5 μm. As for the previous fiber, an indium metal coating was applied to inhibit cladding mode guidance.

The measurement of attenuation on the FTIR spectrometer is made with a shorter length of fiber (≤30 cm) than that realized with monochromatic light

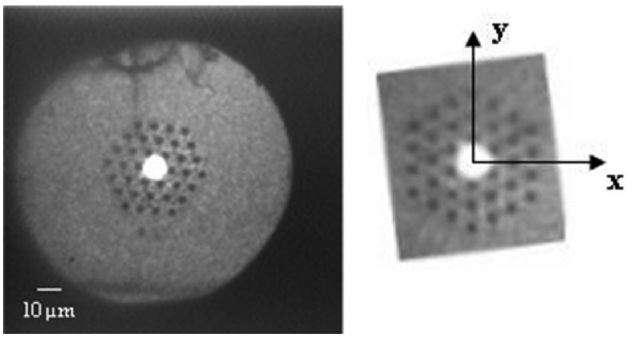

Fig. 6. Near-field observation of the guided beam at 1.55 μm in the MF1

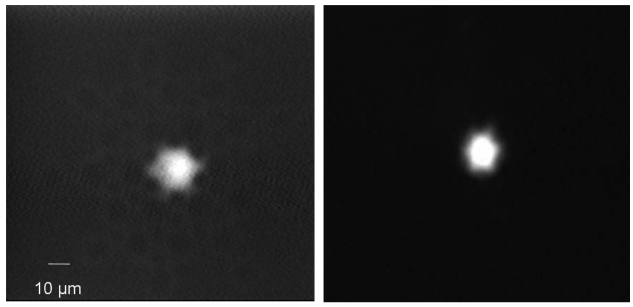

Fig. 7. Near-field observation of the guided beam at 1.55 μm with indium coating.

at 1.55 μm, with a shorter cutback length, perhaps explaining the difference of the attenuation value at 1.55 μm between these two measurements (see Fig. 9). The absorption band centered on 2.9 μm is due to OH absorption. The peaks at 2.05 and 3.1 μm are due to resonances from the main SH absorption peak at 4.1 μm (see Fig. 2). Figure 9 shows that between 2.3 and 2.7 μm the losses are below 12 dB/m.

Figure 10 shows the profile of the output beam at 1.55 μm for the MF2b fiber. Using a Gaussian approximation, experimental measurements give a mode field diameter (MFD) of 3.5 μm for the x axis and 3.3 μm for the y axis. The corresponding computed values are, respectively, 3.7 μm and 3.5 μm, giving a relative error between experimental and computed values of less than 6%. The losses at 1.55 μm for this fiber are 34 dB/m. The computed losses for the fundamental mode at the same wavelength are found to be around 17.5 dB/m without material losses and around 22.3 dB/m with them. We were not able to excite the second mode using the same method as for MF1. We refer to Section 6 for the discussion of these results.

6. Discussion

Here we discuss the origins of the overall losses in the different fibers shown in the previous sections. This issue is crucial since the losses are the current limiting factor of our MF. Next, we briefly compare our results with the ones obtained with soft-glass MFs. We conclude by the determination of the nonlinear parameter of the chalcogenide small-core MF described in the Section 5. The results presented here and previous reports [10] show that the "Stack & Draw" technique is a valid method for the fabrication of chalcogenide MFs of at least up to three rings. Some difficulties must still be overcome to obtain a regular microstructure: homogeneity in hole diameters and control of the interstitial holes. We now control the size of the holes by a gas setup system linked to the preform, but the jacketing step and the use of a glass with excellent thermomechanical properties remain the keys for total control of the profile and of the overall losses.

Measurements show an important difference of loss level between the initial material losses

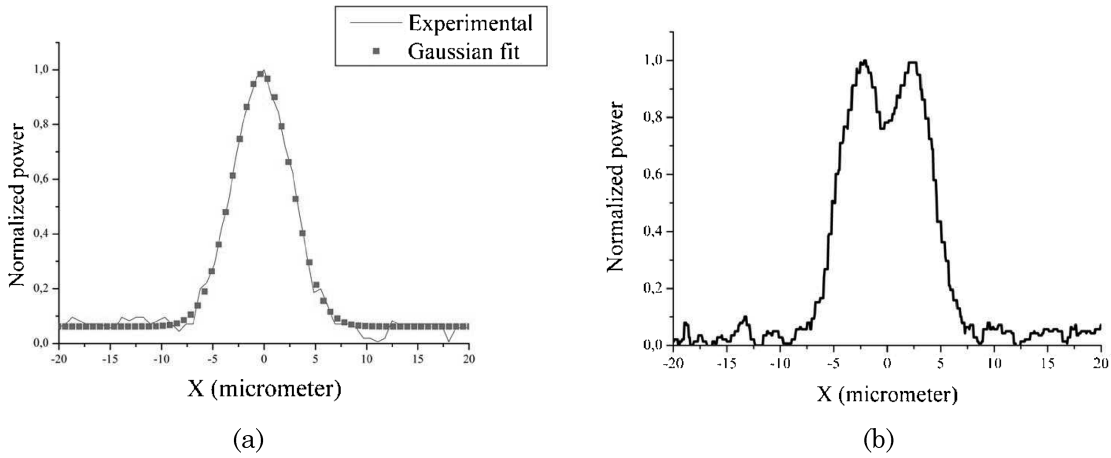

Fig. 8. Experimental profiles at 1.55 μm m in the MF1.

(4.26 dB/m at 1.55 μm, see the last paragraph of Section 3) and the MF ones, 13 dB/m for MF1 and 15 dB/m for MF2a at the same wavelength. The difference is greater for MF2b, 34 dB/m at 1.55 μm. To reduce the losses for future MFs, the results obtained from numerical simulations are useful to understand these discrepancies. They clearly indicate that the limiting factor for the fundamental mode losses of MF1 and MF2a is the material loss. For the second mode of MF1, the scenario is the same: the guiding losses alone are around 0.15 dB/m, and the overall losses reach 4.57 dB/m when material loss is considered. No second mode experimental losses are available but we can expect that they are slightly more important than those of the fundamental mode as suggested by the numerical simulations.

For MF2b, the calculated guiding losses are equal to 17.5 dB/m for the fundamental mode and around 9100 dB/m for the second one. When the material losses are taken into account the fundamental mode, losses are equal to 22.3 dB/m, whereas the measured losses are 34 dB/m. For the second mode, the computed losses with a lossy material are around 9105 dB/m. Consequently, even if the second mode is only starting to delocalize in the microstructured region [23–25], the loss ratio between the two modes explains why the second mode was not found experimentally in MF2b. The MF2b is effectively single-mode for any practical purpose. The easiest way to reduce the fundamental mode losses for future small-core MFs is to decrease the guiding losses. If a similar fiber to MF2b is considered but with a complete third ring of holes (see Fig. 5) then the guiding loss is decreased to 0.11 dB/m. With the material losses taken into account, the overall loss would reach 4.36 dB/m for the fundamental mode, which is equal to the level obtained from the numerical simulation for MF1 and MF2a. For the second mode with the same conditions, the calculated loss is 4000 dB/m. As a result, it should be possible using the same synthesis and drawing processes to get a small-core single-mode chalcogenide MF with overall losses around 15 dB/m found for MF2a at 1.55 μm. Further increase in the number of hole rings is unnecessary since, in this case, the overall loss of the fundamental mode is set by the material loss of 4.35 dB/m, while the addition of a fourth ring of holes would decrease the second mode loss to 2266 dB/m.

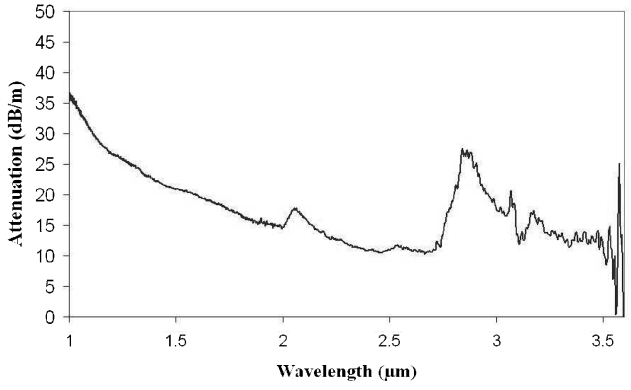

Fig. 9. Attenuation curve of MF2a between 1 and 3.5 μm.

We now discuss the excess loss compared to the computed loss even when homogeneous material loss is considered. This excess is probably due to interface problems between the capillaries during the different drawing steps. These problems are characterized by scattering centers (bubbles or crystals), local glass inhomogeneity, and a non total mixing of the glass at the interfaces that induce diffusion, especially at low wavelengths. Indeed, we observe that when interstitial holes are present in the preform, especially around the core, the losses tend to decrease. This is because the presence of these holes diminishes the surface of glass–glass interfaces. Another source of optical losses can be the photosensitivity of germanium sulphide glasses, including photorefraction and photoinduced anisotropy under sub-bandgap excitation [26].

For soft glasses, the measured losses are 10 dB/m at 1.55 μm for a MF made of the SF-57 Schott glass [27] and slightly above 4 dB/m at the same wavelength for a MF made of the SF-6 Schott glass [28]. Another study on TeO_2-based fibers has shown

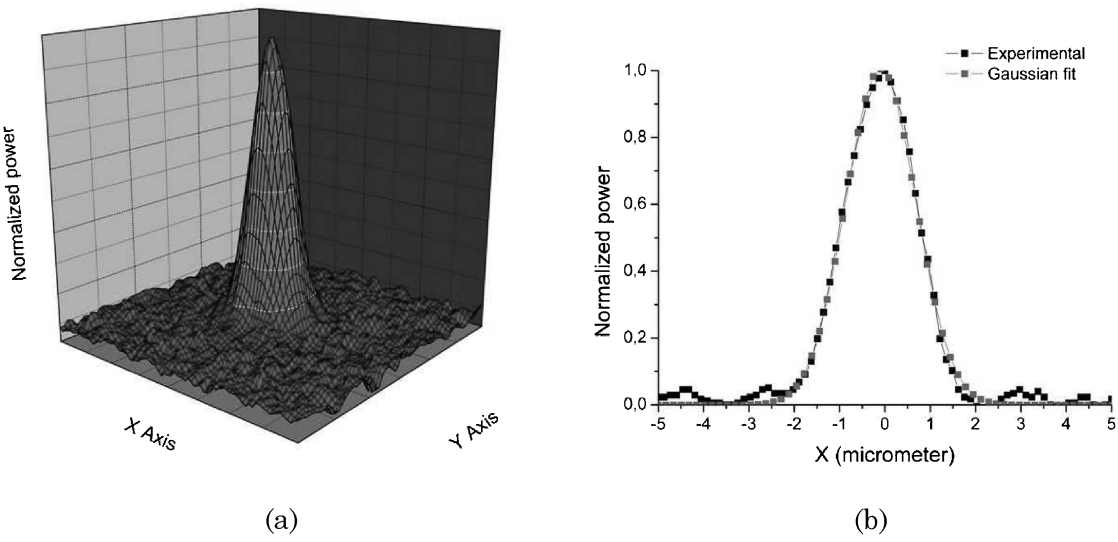

Fig. 10. Experimental profiles of the output beam at 1.55 μm m in the small-core fiber MF2b.

optical losses around 4.5 dB/m at 1.55 μm [29]. These losses are lower than the ones reported in the present study at the same wavelength for the MFs. Nevertheless, the chalcogenide MFs are promising due to their high nonlinear optical properties. Furthermore, these soft glasses have higher losses than the 2SG glass for wavelengths above 2.5 μm. The losses of our 2SG rod are 2.4 dB/m at 2.5 μm and the measured losses of our MF2a fiber are below 12 dB/m bewteen 2.3 and 2.7 μm (see Fig. 9).

To end this discussion, we evaluate the nonlinear parameter of the small-core fiber MF2b. Since the fundamental mode is well confined in the chalcogenide matrix, we can use the formula $\gamma = 2\pi n_2/(\lambda A_{\text{eff}})$ [20]. The effective area A_{eff} is around 10 μm^2. We note that this effective area is seven times smaller than that already obtained in [10]. Since n_2 is around 10^{-18} m^2/W, γ is approximately equal to 1.3 W^{-1} m^{-1}. This value is much smaller than the maximal theoretical γ computed recently for an As_2Se_3 conventional fiber taper [30]. Nevertheless, if we take into account the lengths L of the devices, the comparison is more favorable. We are able to get meter-long small-core MF, therefore the product $(\gamma L)_{\text{MF}}$ is equal to 1.3 W^{-1}, whereas for the taper length L is around 20 mm, giving a product $(\gamma L)_{\text{taper}}$ equal to 3.3 W^{-1}. For future nonlinear devices, MFs have several advantages. First, the MF can be made polarization-maintaining; as a result the nonlinear parameter can be multiplied by a factor 9/8 as explained in Appendix B of [20]. Second, the MF profile can be designed to manage chromatic dispersion [31,32] to obtain an anomalous dispersion regime at the sought wavelength. Third, several meters of regular and reproducible MF can be obtained using the standard "Stack & Draw" process.

7. Conclusion

Several 2SG chalcogenide MFs with regular profile have been fabricated with the "Stack & Draw" process. For the first time, to the best of our knowledge, a small-core (4 μm) chalcogenide MF with single-mode behavior, at least at 1.55 μm, has been obtained. All the described fibers have been optically characterized. The numerical results concerning the MFD are in good agreement with the experimental data. Concerning optical losses, the numerical results are coherent with the measured results. Comparison between the two has allowed us to optimize the future small-core MF profile to reduce the overall losses. A challenging task will be the further reduction of material loss and the supplementary losses induced by capillary surface problems. Success in these tasks will enable a reduction of the overall loss level for chalcogenide MF to below 3 dB/m, which will open up new opportunities in nonlinear photonics in fibers. Furthermore, due to their infrared transmittance, the chalcogenide MFs will also be studied to observe nonlinear phenomena above 2 μm.

We acknowledge the French Délégation Générale pour l'Armement (contracts 05.34.053 and 05.34.008) and the French ANR (FUTUR contract) for their financial support.

References

1. T. A. Birks, J. C. Knight, and P. J. S. Russell, "Endlessly single-mode photonic crystal fiber," Opt. Lett. **22**, 961–963 (1997).
2. S. Coen, A. H. L. Chau, R. Leonhardt, J. D. Harvey, J. C. Knight, W. J. Wadsworth, and P. St. J. Russell, "White-light supercontinuum generation with 60 ps pump pulses in a photonic crysral fiber," Opt. Lett. **26**, 1356–1358 (2001).
3. J. K. Ranka, R. S. Windeler, and A. J. Stentz, "Visible continuum generation in air-silica microstructure optical fibers with anomalous dispersion at 800 nm," Opt. Lett. **25**, 25–27 (2000).
4. J. M. Dudley, L. Provino, N. Grossard, H. Maillotte, R. Windeler, B. Eggleton, and S. Coen, "Supercontinuum generation in air-silica microstructured fibers with nanosecond

and femtosecond pulse pumping," J. Opt. Soc. Am. B **19**, 765–771 (2002).
5. J. M. Fini, "Microstructure fibres for optical sensing in gases and liquids," Meas. Sci. Technol. **15**, 1120–1128 (2004).
6. A. S. Webb, F. Poletti, D. J. Richardson, and J. K. Sahu, "Suspended-core holey fiber for evanescent-field sensing," Opt Eng. **46**, 010503 (2007).
7. D. Hewak, ed., *Properties, Processing and Applications of Glass and Rare Earth-Doped Glasses for Optical Fibers*, Vol. 22 of EMIS Datarev. Ser. (INSPEC, 1998).
8. F. Smektala, C. Quemard, V. Couderc, and A. Barthélémy, "Non-linear optical properties of chalcogenide glasses measured by z-scan," J. Non-Cryst. Solids **274**, 232–237 (2000).
9. T. M. Monro, Y. D. West, D. W. Hewak, N. G. R. Broderick, and D. J. Richardson, "Chalcogenide holey fibres," Electron. Lett. **36**, 1998–2000 (2000).
10. L. Brilland, F. Smektala, G. Renversez, T. Chartier, J. Troles, T. Nguyen, N. Traynor, and A. Monteville, "Fabrication of complex structures of holey fibers in chalcogenide glass," Opt. Express **14**, 1280–1285 (2006).
11. J. M. Dudley, G. Genty, and S. Coen, "Supercontinuum generation in photonic crystal fiber," Rev. Mod. Phys. **78**, 1135–1184 (2006).
12. J. S. Sanghera, I. D. Aggarwal, L. B. Shaw, C. M. Florea, P. Pureza, V. Q. Nguyen, F. Kung, and I. D. Aggarwal, "Nonlinear properties of chalcogenide glass fibers," J. Optoelectron. Adv. Mater. **8**, 2148–2155 (2006).
13. C. M. Smith, N. Venkataraman, M. T. Gallagher, D. Müller, J. A. West, N. F. Borrelli, D. C. Allan, and K. W. Koch, "Low-loss hollow-core silica/air photonic bandgap fibre," Nature **424**, 657–659 (2003).
14. A. Bétourné, G. Bouwmans, Y. Quiquempois, M. Perrin, and M. Douay, "Improvements of solid-core photonic bandgap fibers by means of interstitial air holes," Opt. Lett. **32**, 1719–1721 (2007).
15. Crystal Fibre, http://www.crystal-fibre.com/.
16. M. Guignard, V. Nazabal, F. Smektala, J. L. Adam, O. Bohnke, C. Duverger, A. Moreac, H. Zeghlache, A. Kudlinski, G. Martinelli, and Y. Quiquempois, "Chalcogenide glasses based on germanium disulfide for second harmonic generation," Adv. Funct. Mater. **17**, 3284–3294 (2007).
17. M. F. Churbanov, I. V. Scripachev, G. E. Snopatin, V. S. Shiryaev, and V. G. Plotnichenko, "High-purity glasses based on arsenic chalcogenides," J. Optoelectron. Adv. Mater. **3**, 341–349 (2001).
18. J. S. Sanghera, L. E. Busse, and I. D. Aggarwal, "Effect of scattering centers on the optical loss of As_2S_3 glass fibers in the infrared," J. Appl. Phys. **75**, 4885–4891 (1994).
19. J. C. Knight, T. A. Birks, P. St. J. Russel, and D. M. Atkin, "All silica single-mode optical fiber with photonic crystal cladding," Opt. Lett. **21**, 1547–1549 (1996).
20. J. C. Knight, T. A. Birks, P. St. J. Russell, and D. M. Atkin, "All-silica single-mode optical fiber with photonic crystal cladding: errata," Opt. Lett. **22**, 484 (1997).
21. G. P. Agrawal, *Nonlinear Fiber Optics*, 3rd ed. (Academic, 2001).
22. T. M. Monro and D. J. Richardson, "Holey optical fibres: Fundamental properties and device applications," C.R. Physique **4**, 175–186 (2003).
23. G. Renversez, F. Bordas, and B. T. Kuhlmey, "Second mode transition in microstructured optical fibers: Determination of the critical geometrical parameter and study of the matrix refractive index and effects of cladding size," Opt. Lett. **30**, 1264–1266 (2005).
24. F. Zolla, G. Renversez, A. Nicolet, B. Kuhlmey, S. Guenneau, and D. Felbacq, *Foundations of Photonic Crystal Fibres* (Imperial College, 2005).
25. L. Labonté, D. Pagnoux, P. Roy, F. Bahloul, M. Zghal, G. Mélin, E. Burov, and G. Renversez, "Accurate measurement of the cutoff wavelength in a microstructured optical fiber by means of an azimuthal filtering technique," Opt. Lett. **31**, 1779–1781 (2006).
26. V. Tikhomirov, G. J. Adriaenssens, and A. J. Faber, "Photoinduced anisotropy and photorefraction in Pr-doped Ge-Ga-S glasses," J. Non-Cryst. Solids **213–214**, 174–178 (1997).
27. K. M. Kiang, K. Frampton, T. Monro, R. Moore, J. Tucknott, D. W. Newak, D. J. Richardson, and H. N. Rutt, "Extruded single-mode non-silica glass holey optical fibres," Electron. Lett. **38**, 546–547 (2002).
28. V. V. Ravi Kanth Kumar, A. K. George, W. H. Reeves, J. C. Knight, P. St. J. Russell, F. G. Omenetto, and A. J. Taylor, "Extruded soft glass photonic crystal fiber for ultrabroad supercontinuum generation," Opt. Express **10**, 1520–1524 (2002).
29. V. V. Ravi Kanth Kumar, A. K. George, J. C. Knight, and P. St. J. Russell, "Tellurite photonic crystal fiber," Opt. Express **11**, 2641–2645 (2003).
30. E. C. Mägi, L. B. Fu, H. C. Nguyen, M. R. Lamont, D. I. Yeom, and B. J. Eggleton, "Enhanced Kerr nonlinearity in subwavelength diameter As_2Se_3 chalcogenide fiber tapers," Opt. Express **15**, 10324–10329 (2007).
31. B. Kuhlmey, G. Renversez, and D. Maystre, "Chromatic dispersion and losses of microstructured optical fibers," Appl. Opt. **42**, 634–639 (2003).
32. G. Renversez, B. Kuhlmey, and R. McPhedran, "Dispersion management with microstructured optical fibers: Ultra-flattened chromatic dispersion with low losses," Opt. Lett. **28**, 989–991 (2003).